Review

Effect of silver doping on the TiO_2 for photocatalytic reduction of CO_2

K. Kočí [a,*], K. Matějů [a], L. Obalová [a], S. Krejčíková [b], Z. Lacný [a], D. Plachá [a], L. Čapek [c], A. Hospodková [d], O. Šolcová [b]

a Technical University of Ostrava, 17. listopadu 15, Ostrava, Czech Republic
b Institute of Chemical Process Fundamentals of the ASCR, v.v.i., Rozvojová 135, Prague, Czech Republic
c University of Pardubice, Faculty of Chemical Technology, Studentská 95, Pardubice, Czech Republic
d Institute of Physics of the ASCR, v.v.i., Na Slovance 2, Praha 8, Czech Republic

ARTICLE INFO

ABSTRACT

Pure TiO_2 and various silver-enriched TiO_2 powders were prepared by the sol–gel process controlled in the reverse micellar environment. The catalysts were tested in CO_2 photocatalytic reduction and characterized by X-ray diffraction (XRD), nitrogen adsorption measurement and UV–vis. Methane and methanol were the main reduction products. The yield of methane and methanol increases when modifying the TiO_2 by silver incorporation is caused by two mechanisms: up to 5% of Ag in TiO_2 the Ag impurity band inside the TiO_2 bandgap decreases the absorption edge and increases so the electron–hole pair generation, above 5% of Ag in TiO_2 Ag metallic clusters are formed in TiO_2 crystals with Shottky barrier at the metal–semiconductor interface, which spatially separates electron and holes and increases their lifetime (decreases probability of their recombination).

Contents

1. Introduction

The atmospheric concentrations of greenhouse gases, i.e. CO_2, CH_4, N_2O, O_3 and CFCs have been reported to increase dramatically. The concern about human-induced climate change grows out of the increasing atmospheric concentrations of these greenhouse gases. Carbon dioxide (CO_2) is supposed to be the most important greenhouse gas; therefore the reduction of CO_2 is an issue drawing the attention of many researchers. The reduction of CO_2 by photocatalysts is one of the most promising methods since CO_2 can be reduced to useful compounds by irradiating it with UV light at room temperature and ambient pressure.

The advantages of titania photocatalysts, such as strong resistance to chemical and photocorrosion, low operational temperature, low cost, significantly low energy consumption, have led to the relevant applications of the photocatalytic reduction of CO_2 [1–26]. However, TiO_2 exhibits a relatively high energy bandgap (3.2 eV) and can only be excited by high energy UV irradiation with a wavelength shorter than 387.5 nm. Efforts have been made to extend the light absorption range of TiO_2 from UV to visible light and to improve the photocatalytic activity of TiO_2 further by adding noble metals. For example, Ag can serve as successful dopant to TiO_2

* Corresponding author. Tel.: +420 596991592.
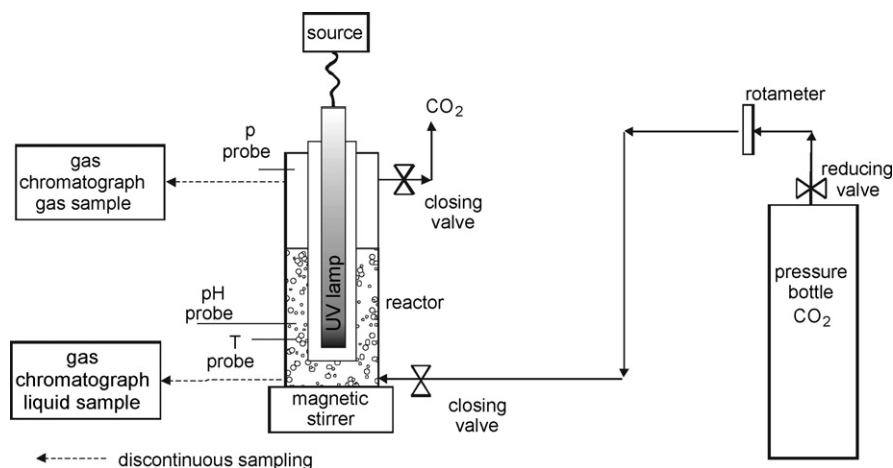E-mail address: kamila.koci@vsb.cz (K. Kočí).

Fig. 1. Block scheme of the apparatus for CO_2 photocatalytic reduction.

for increasing yields of several types of photocatalytic reactions [29–39].

Chang et al. [27,28] prepared nanocrystalline Ag/TiO_2 composite thin films by a sol–gel spin coating technique. The photocatalytic properties of the prepared thin films were evaluated by degrading methylene blue under UV. By making the TiO_2 film porous and adding the Ag element, the photocatalytic performance of the TiO_2-based thin films can be improved significantly.

Colmenares et al. [29] probed the photocatalytic activity of TiO_2 doped with diverse transition metals (Ag, Fe, Pd, Pt, Zn and Zr) synthesized by the sol–gel method. All the solids were tested for gas phase selective photooxidation of 2-propanol. Doping with Pd, Pt or Ag resulted in an increase in molar conversion compared to bareTiO_2.

Vamathevan et al. [30] investigated the photocatalytic oxidation of sucrose in the presence of dissolved Fe^{3+} and Ag^+ ions in titanium dioxide suspensions under near-UV illumination. The oxidation of sucrose to carbon dioxide was enhanced in the presence of these metal ions. An optimum metal ion loading was observed for silver (2.0 mol%). The role of metal ions in photocatalytic reactions is a function of the type of metal and its concentration in the system.

Sobana et al. [31,32] examined the photocatalytic degradation of two direct diazo dyes, direct red 23 (DR 23) and direct blue 53 (DB 53) in the aqueous suspensions of TiO_2 and Ag deposited TiO_2 nanoparticles under UV-A light irradiation in order to evaluate the various effects of silver deposition on the photocatalytic activity of TiO_2. The presence of silver in TiO_2 was found to enhance the photodegradation of DR 23 and DB 53. The photonic efficiency increases along with the increase in metal loading up to an optimum level. The higher activity of silver-doped TiO_2 is due to the enhancement of electron–hole separation by the electron trapping of silver particles.

Lee et al. [33] evaluated the photocatalytic activity of TiO_2 powder samples by degradation of 1,4-dichlorobenzene (DCB). Silver was deposited on TiO_2 powders (Degussa P25) by the photodecomposition of two different silver salts, AgF and $AgNO_3$. They observed that the photocatalytic activity of Ag-loaded TiO_2 films was greater than that of pure TiO_2 films.

Seery et al. [34] described the synthesis of TiO_2 containing different amounts of silver by the sol–gel route. The synthetic method where the silver nitrate was not reduced by light before calcination resulted in a slightly more efficient photocatalysis over the method where it was reduced. All materials with added silver showed visible light activation in both the Q-Sun solar simulator and Dublin sunlight the activity was increasing with increasing amounts of silver.

Sahoo et al. [35] monitored the photocatalytic degradation of methyl red dye in aqueous solutions under UV irradiation using Ag^+ doped TiO_2. The dye degradation was more efficient in case of Ag^+ doped TiO_2.

Chao et al. [36] found that the Ag doping promotes the phase transformation but has a depressing effect on the anatase grain growth. With a suitable amount (ca. 2–6 mol%), the Ag dopant reduces the anatase grain size and increases the specific surface area of the TiO_2 powder, which exhibits a great potential in improving the TiO_2 photocatalytic activity.

Iliev et al. [37] modified the commercially available TiO_2 catalyst (Degussa P25) with nanosized platinum and silver particles by the photoreduction method to obtain a different noble metal loading (0.5 and 1 wt.%). The degradation of oxalic acid has been studied in aqueous solution photocatalyzed by irradiated TiO_2 modified with nanosized silver particles. The photocatalytic activity of TiO_2, modified with noble metal, is approximately double that of the semiconducting support. The increase of the quantum yield of the photodestruction reaction of the studied model pollutant is due to the formation of Schottky barriers on the metal–semiconductor interface, which serve as efficient electron traps, preventing the electron–hole recombination.

Noble metals doped or deposited on TiO_2 are expected to show various effects on the photocatalytic activity of TiO_2 by different mechanisms. These noble metals act separately or simultaneously depending on the photoreaction conditions. They may (i) enhance the electron–hole separation due to Schottky barrier formation, (ii) extend the light absorption into a visible range and enhance surface electron excitation by plasmon resonances excited by visible light and (iii) modify the surface properties of photocatalysts [32].

As the effect of Ag dopant in TiO_2 on the efficiency of CO_2 photocatalytic reduction has not been studied yet, in the presented article the photocatalytic reduction of carbon dioxide is studied in the presence of silver-modified TiO_2. The aim of the study is to investigate the influence of the silver dopant TiO_2 on the yields in both phases (liquid and gas). The main products of the photocatalytic process methane in gas phase and methanol in liquid phase are expected according to earlier researchers [1,4,5,16].

2. Experimental

2.1. Ag/TiO₂ preparation

Pure TiO_2 and various silver-enriched TiO_2 powders were prepared by the sol–gel process controlled in the reverse micellar environment. Pure TiO_2 was synthesized by the addition of Tita-

Table 1
Basic characterisation of prepared samples.

| Sample	TiO_2	1% Ag–TiO_2	3% Ag–TiO_2	5% Ag–TiO_2	7% Ag–TiO_2
Content Ag[a] [wt.%]	0.00	0.725	2.37	3.38	5.19
S_{BET} [m²/g]	67.6	79.8	82.4	80.0	79.7
r_{max}[b] [nm]	1.48	1.41	1.48	1.41	1.65
Absorption edge [eV]	2.98	2.88	2.84	2.75	2.74

[a] Determined by XRF.
[b] Maximum pore radius.

nium (IV) isopropoxide (Ti(OCH(CH$_3$)$_2$)$_4$, Aldrich, 99.999%) into formed inverse micellar solution made of cyclohexane (Aldrich, 99.9+%, HPLC grade), nonionic surfactant Triton X-114 (C$_{27}$H$_{48}$O$_{7.5}$, Aldrich) and distilled water. The molar ratio of cyclohexane:Triton X-114:water:Ti(OC$_3$H$_7$)$_4$ was kept at 11:1:1:1 (volume ratio TX-114:cyclohexane = 0.49) [38]. The beaker with the solution made of appropriate amount of cyclohexane, Triton X-114 and water was stirred intensively for 15 min for homogenization and formation of inverse micelles. Then liquid Titanium (IV) isopropoxide was regularly dropped into the micellar solution during the vigorous stirring. During the addition of isopropoxide drop by drop the sol changed the state from transparent to viscous yellow. After the addition of all the isopropoxide the sol was stirred for another 10 min. Lastly, the sol was left in a bowl exposed to air for 24 h. The obtained rigid gel was calcined at 400 °C for 4 h with the temperature ramp 1 °C/min in an air flow in a muffle furnace. Various Ag-enriched TiO$_2$ powders were prepared analogically, however AgNO$_3$ (Aldrich, 99.9999%) solution of suitable concentration (0.25 M, 0.75 M, 1.3 M and 1.85 M) was added instead of distilled water.

2.2. Characterization of TiO$_2$ catalysts

The surface area and porous structure of prepared catalysts were evaluated from nitrogen adsorption isotherms by the BET and BJH methods, respectively. Nitrogen physical adsorption was performed on a volumetric apparatus ASAP2020 Micromeritics (USA). Before analyses the samples were dried at 105 °C for 24 h in vacuum (0.1 Pa).

UV–vis diffuse reflectance spectra of samples were recorded using GBS CINTRA 303 spectrometer equipped with a diffuse reflectance attachment with a spectralon-coated integrating sphere against spectralon reference. The reflectances were re-calculated to the absorption using the Schuster–Kubelka–Munk equation, $F(R_\infty) = (1 - R_\infty)^2 / 2R_\infty$, where R_∞ is the diffuse reflectance from a semi-infinite layer. Absorption edge was estimated by extrapolating the decreasing portion of the spectrum to the abscissa at zero absorption.
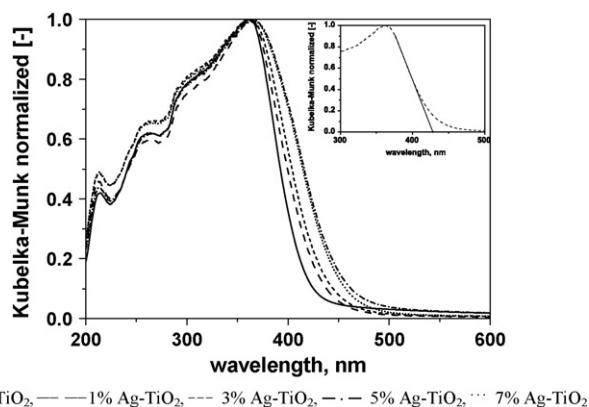
Ag-to-TiO$_2$ mass ratio in Ag/TiO$_2$ powders were determined by X-ray fluorescence (XRF) analysis using an ARL 9400 XP sequential WD-XRF spectrometer with the standard deviation lower than 5%.

The purity (carbon content in weight %) of the powders was specified on an Elementar Vario EL III (Elementar). The detection limit of the apparatus was 0.1 wt.%.

XRD powder diffraction patterns were obtained with the aid of a Seifert-FMP or a Panalytical-MPD laboratory diffractometer with Cu Kα radiation in the conventional focusing Bragg–Brentano geometry in the diffraction angle range 2Θ = 10–90°.

2.3. Photocatalytic reactivity experiments

The photocatalytic reduction of carbon dioxide was carried out in a homemade apparatus (Fig. 1).

The photocatalytic reduction of carbon dioxide was carried out in a stirred batch annular reactor with a suspended catalyst illuminated by UV 8 W Hg lamp (254 nm). GC/FID/TCD was used for the analysis of gas and liquid reaction products. The details of the photocatalytic CO$_2$ reduction experiment and analytical methods were described in our previous publication [39]. It is important to minimize the influence of transport phenomena during kinetic measurements. The elimination of CO$_2$ diffusion from the bulk of gas through the gas–liquid interface in a laboratory batch slurry reactor was accomplished by saturating the liquid with pure CO$_2$ before the reaction had been started [4,11]. Catalyst loading of 1 g dm^{-3} was chosen to avoid concentration gradients in the bulk of stirred liquid with TiO$_2$ suspension due to the scattering effect of light caused by the high TiO$_2$ concentration [11,16,40,41]. The determination of suitable volume of the liquid phase in our annular photoreactor to fulfil the requirement of perfect mixing has been published recently as 100 ml [42].

The accuracy of measurements was verified by series of repeated measurements. Average values were mentioned in this article. Maximal relative error was 5%.

3. Results and discussion

3.1. Characterization of TiO$_2$ nanoparticles

The basic textural properties of prepared titania and doped titania samples are summarised in Table 1 together with real Ag content determined by XRF. All samples possess a relatively high surface area; moreover, the positive effect of silver, which increases the surface area by about 15%, is clearly noticeable. It is obvious that the surface areas of Ag-doped TiO$_2$ samples varied only slightly and they are independent on the growth of Ag amount. The pore maxima of all samples are nearly the same without dependence on the Ag presence.

The purity of all prepared samples was excellent, because the organic residual content was lower than 0.1 wt.%.

XRD analysis confirmed the presence of the pure anatase crystallite structure for all samples. Ag was not detected in XRD pattern, probably Ag is situated in the bulk (inside the TiO$_2$ crystals) and/or Ag clusters are smaller than 0.3 nm.
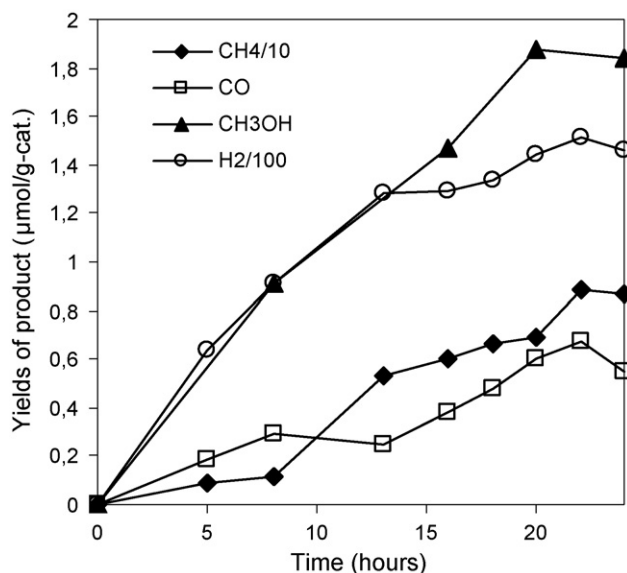

Fig. 2. UV–vis spectrum of prepared Ag–TiO$_2$ catalysts, insert: the illustration as the value of absorption edge was achieved.

— TiO$_2$, — 1% Ag–TiO$_2$, --- 3% Ag–TiO$_2$, — · — 5% Ag–TiO$_2$, ··· 7% Ag–TiO$_2$

Fig. 3. Time dependence of the product concentrations over the 7% Ag–TiO₂ catalysts.

Fig. 4. Time dependence of methane yields over the Ag-modified TiO₂ catalysts.

Fig. 2 shows the UV–vis spectra of Ag–TiO₂ catalysts. It is seen that (i) the maxima of the UV–vis band increased with the increasing Ag loading from 360 to 367 nm and (ii) the maximum absorption wavelength increased with increasing Ag loading, i.e. the absorption was shifted into the visible region for Ag–TiO₂ catalysts and the shift increased with the increasing amount of silver. The absorption edge (Fig. 2) values are given in Table 1.

3.2. The photocatalytic reduction of CO₂

The effect of irradiation time on the formation of CO_2 photocatalytic reduction products was investigated over a period of 0–24 h on TiO₂ catalysts with different amount of Ag. Fig. 3 shows the evolution of all reaction products as the functions of the irradiation for a 7% Ag–TiO₂ catalyst. Two main products were determined: methane in the gas phase and methanol in the liquid phase. Hydrogen and low amounts of carbon monoxide were also detected. Other products such as formic acid, formaldehyde, ethane and ethylene could also be formed [2,16], but they were undetectable. The observed order of yields ($\mu mol/g_{cat}$) order was: $H_2 > CH_4 > CH_3OH \geq CO$.

We assume on the basic of observed products the mechanism where the formation of carbon monoxide from $•CO_2^-$ radical is the first step. Then both methane and methanol are formed in the parallel reactions. This mechanism was first suggested by Anpo [3]. Several authors [2,5,17] proposed the same mechanism with the exception that they predicted the formation of a carbon radical instead of surficial carbon.

$$CO_2 \longrightarrow CO \nearrow^{CH_4}_{\searrow CH_3OH}$$
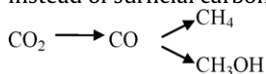
Comparisons of CH₄, CH₃OH, H₂ and CO yields over TiO₂ with different Ag content are shown in Figs. 4–6A and B respectively. The yields of methane were negligible during the first 8 h of irradiation in all cases with the exception of catalyst 1 and 5% Ag-TiO₂ (Fig. 4). A similar trend of yield-time dependency was observed; only the shape for the sample with 7% Ag–TiO₂ was slightly different. A substantial increase of methane yield was observed after 8 h of irradiation. The highest yield of methane was observed for 7% Ag–TiO₂ catalyst.

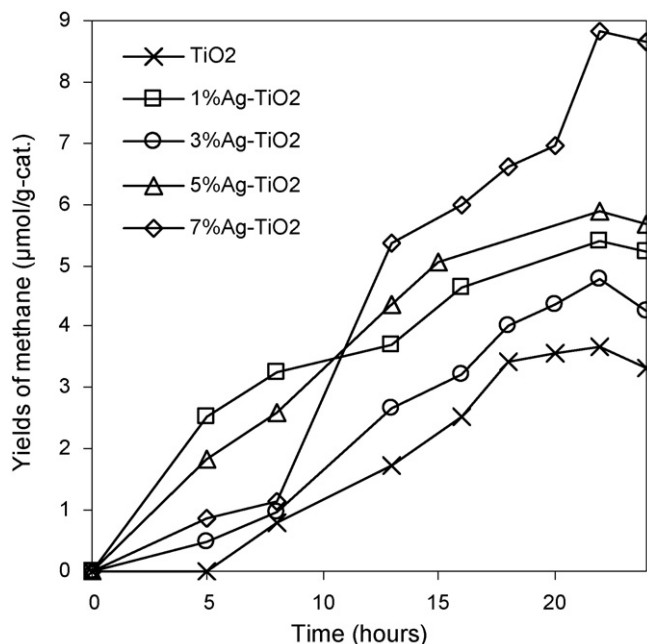The yields of methanol were one order of magnitude lower than the yields of methane (Fig. 5). Data at 5 h were measured but were under the limit of determinableness (12 μg/l i.e. 0.38 μmol/g-catalyst). The steepest curve of methanol yield was measured for the 7% Ag–TiO₂ catalyst.

The hydrogen yields were small during the first 13 h of irradiation in all cases (Fig. 6A). After 15 h the hydrogen yields started increasing slowly. The yields of carbon monoxide increased slowly during the reaction but all yields were near the limit of detection (Fig. 6B).

The data from the longest reaction time span were chosen for the comparison because the yields of all products were the highest and the most accurate. The effect of silver doping on the yields
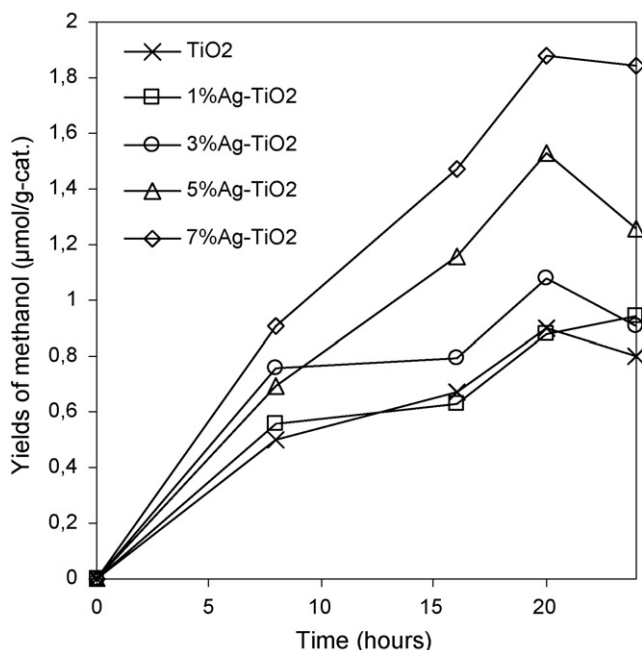

Fig. 5. Time dependence of methanol yields over the Ag-modified TiO₂ catalysts.
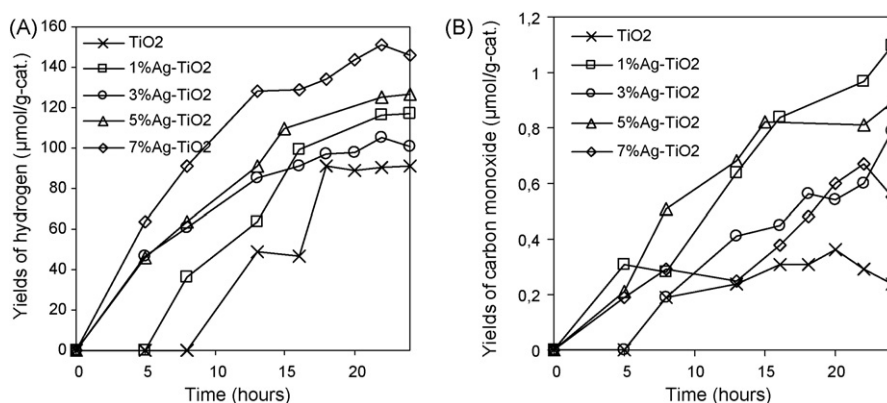
Fig. 6. (A and B) Time dependence of the hydrogen (A) and the carbon monoxide (B) yields over the Ag-modified TiO_2 catalysts.

of the two main products (methane and methanol) related to the weight of the catalyst is depicted in Fig. 7. The photoreactivity of Ag-TiO$_2$ increases with the increase in the Ag dopant concentration. Both yields are the highest for 7% Ag–TiO$_2$. The effect of the Ag dopant on the CO_2 photocatalytic reduction has not been studied yet. However, an optimum amount of Ag corresponding to the highest product yields was found for other photocatalytic reactions [27,28,34,36].

The yields of the two main products (methane and methanol) expressed per 1 m^2 of catalyst surface (Fig. 8) show similar trends with the highest yields obtained for 7% Ag–TiO$_2$. This indicates that the specific surface area is not the most decisive parameter in the CO_2 photocatalytic reduction.

Doping with metals or metal oxides could cause two effects:

(1) Firstly, it creates impurity band inside the TiO$_2$ bandgap, thus shifting the absorption edge to the visible region [29]. The decrease of the absorption edge and the shift of absorption wavelength into the visible region in this paper are clearly visible from Table 1 and Fig. 2, for Ag content up to 5%. The decrease of the absorption edge increases the electron and hole

pair photogeneration, which causes yields increase of CO_2 photoreduction.

(2) Secondly, for Ag content above 5% silver atoms are not anymore randomly located in TiO$_2$ crystal, but forms probably metallic clusters inside TiO$_2$ crystal. These metal clusters could provoke a decrease in the electron–hole recombination rate [43,44]. This hypothesis was based on the fact that the Fermi level of TiO$_2$ is higher than that of silver metals [45]. Such phenomenon would be expected to lead to the formation of a Schottky barrier at metal–semiconductor contact region, which causes the charge separation, the decrease of electron–hole recombination rate and consequently increase of the TiO$_2$ photocatalytic activity. The above mentioned fact could be the reason for observed yields increases with increased Ag content in our experiments with CO_2 photocatalytic reduction and is the main reason of yields increase with 7% Ag–TiO$_2$ since the absorption edge has same value as 5% Ag–TiO$_2$.

Our results are in agreement with other works dealing with photocatalytic activity of Ag-doped TiO$_2$. For example, the presence of Ag in TiO$_2$ increased the yield of dye degradation [27,28,31,32], photooxidation of 2-propanol [29], degradation
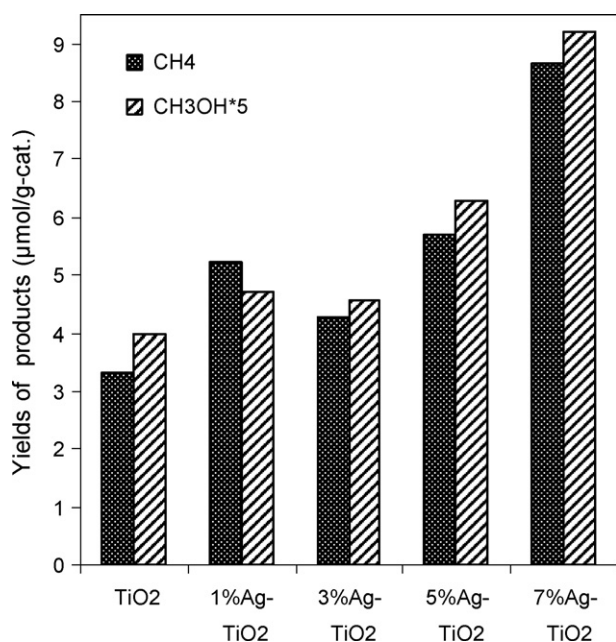

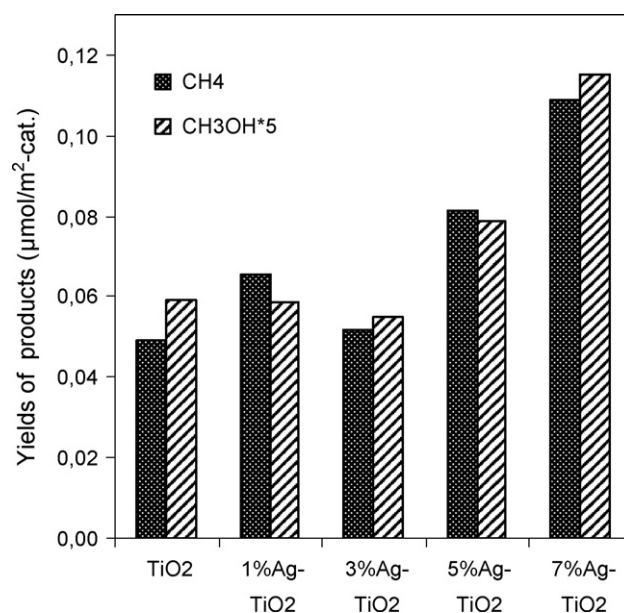**Fig. 7.** Dependence of the product yields (after 24 h of irradiation) on the different catalysts.

Fig. 8. Dependence of the product yields related to specific surface area (after 24 h of irradiation) on the different catalysts.

of 1,4-dichlorobenzene [33] and degradation of oxalic acid [37].

4. Conclusion

The photocatalytic properties of the prepared nanocrystalline Ag–TiO$_2$ catalysts were evaluated by photocatalytic reduction of CO$_2$. A slight increase of specific surface area was observed for the Ag-modified samples compared to that of pure TiO$_2$. It would be expected that the Ag-doped sol–gel TiO$_2$ powder should possess higher photocatalytic activity. However, the main factor which influenced the yields of CO$_2$ photocatalytic reduction is not the specific surface area but the Ag content. The yield increase of the redox process when modifying the TiO$_2$ with silver is mainly caused by two mechanisms: first, by more effective electron hole pair generation due to shift of absorption edge towards visible light in case of random dissipation of Ag atoms into TiO$_2$ crystals (up to 5%) and secondly, due to the formation of a Schottky barrier at the metal–semiconductor interface around Ag metallic clusters (formed above 5% of Ag in TiO$_2$), which causes spatial separation of electrons and holes and decreases their recombination rate.

The reduction of CO$_2$ by photocatalysts was one of the most promising methods, since CO$_2$ can be reduced to useful compounds by irradiating it with UV light. However, the efficiency of this method was relatively low and an increase of yield is necessary.

Acknowledgements

References

[1] K. Hirano, K. Inoue, T. Yardu, J. Photochem. Photobiol. A: Chem. 64 (1992) 255–258.
[2] K. Adachi, K. Ohta, M. Mizuno, Sol. Energy 53 (1994) 187–190.
[3] M. Anpo, H. Yamashita, Y. Ichihashi, S. Ehara, J. Electroanat. Chem. 396 (1995) 21–26.
[4] T. Mizuno, K. Adachi, K. Ohta, A. Saji, J. Photochem. Photobiol. A: Chem. 98 (1996) 87–90.
[5] S. Kaneco, Y. Shimizu, K. Ohta, T. Mizuno, J. Photochem. Photobiol. A: Chem. 115 (1998) 223–226.
[6] B.-J. Liu, T. Torimoto, H. Yoneyama, J. Photochem. Photobiol. A: Chem. 115 (1998) 227–230.
[7] H. Yamashita, Y. Fijuu, Y. Ichihashi, S.G. Zhang, K. Ikeue, D.R. Park, K. Koyano, T. Tatsumi, M. Anpo, Catal. Today 45 (1998) 221–227.
[8] M. Subrahmanyam, S. Kaneco, N. Alonso-Vante, Appl. Catal. B: Environ. 23 (1999) 169–174.
[9] K. Kaneco, H. Kurimoto, Y. Shimizu, K. Ohta, T. Mizuno, Energy 24 (1999) 21–31.
[10] Y. Kohno, H. Hayashi, S. Takenaka, T. Tanaka, T. Funabiki, S. Yoshida, J. Photochem. Photobiol. A: Chem. 126 (1999) 117–124.
[11] I.-H. Tseng, W.-C. Cheng, J.C.S. WU, Appl. Catal. B: Environ. 37 (2002) 37–48.
[12] I.-H. Tseng, J.C.S. Wu, H.-Y. Chou, J. Catal. 221 (2004) 432–440.
[13] G.R. Dey, A.D. Belapurkar, K. Kishore, J. Photochem. Photobiol. A: Chem. 163 (2004) 503–508.
[14] J.C.S. Wu, H.-M. Lin, C.-L. Lai, Appl. Catal. A: Gen. 296 (2005) 194–200.
[15] Slamet, H.W. Nusation, E. Purnama, S. Kosela, J. Gunlazuardi, Catal. Commun. 6 (2005) 313–319.
[16] N. Sasirekha, S.J.S. Basha, K. Shanthi, Appl. Catal. B: Environ. 62 (2006) 169–180.
[17] S.S. Tan, L. Zou, E. Hu, Catal. Today 115 (2006) 269–273.
[18] S.S. Tan, L. Zou, E. Hu, Sci. Technik. Adv. Mater. 8 (2007) 89–92.
[19] X.-H. Xia, Z.-J. Jia, Y. Yu, Y. Liang, Z. Wang, L.-L. Ma, Carbon 45 (2007) 717–721.
[20] S. Liu, Z. Zhao, Z. Wang, Photochem. Photobiol. Sci. 6 (2007) 695–700.
[21] C.-C. Lo, C.-H. Hung, C.-S. Yuan, J.-F. Wu, Sol. Energy Mater. Sol. Cells 91 (2007) 1765–1774.
[22] T.-V. Nguyen, J.C.S. Wu, Sol. Energy Mater. Sol. Cells 92 (2008) 864–872.
[23] Q.-H. Zhang, W.-D. Han, Y.-J. Hong, J.-G. Yu, Catal. Today 148 (2009) 335–340.
[24] Z. Zhao, J. Fan, M. Xie, Z. Wang, J. Clean. Product 17 (2009) 1025–1029.
[25] O.K. Varghese, M. Paulose, T.J. LaTempa, C.A. Grimes, Nano Lett. 9 (2009) 731–737.
[26] J.C.S. Wu, Catal. Surv. Asia 13 (2009) 30–40.
[27] Ch.-Ch. Chang, Ch.-K. Lin, Ch.-Ch. Chan, Ch.-S. Hsu, Ch.-Y. Chen, Thin Solid Films 494 (2006) 274–278.
[28] Ch.-Ch. Chang, J.-Y Chen, T.-L. Hsu, Ch.-K. Lin, Ch.-Ch. Chan, Thin Solid Films 516 (2008) 1743–1747.
[29] J.C. Colmenares, M.A. Aramendía, A. Marinas, J.M. Marinas, F.J. Urbano, Appl. Catal. A: Gen. 306 (2006) 120–127.
[30] V. Vamathevan, H. Tse, R. Amal, G. Low, S. Mcevoy, Catal. Today 68 (2001) 201–208.
[31] N. Sobana, M. Muruganadham, M. Swaminathan, J. Mol. Catal. A: Chem. 258 (2006) 124–132.
[32] N. Sobana, K. Selvam, M. Swaminathan, Sep. Purif. Technik. 62 (2008) 648–653.
[33] M.S. Lee, S.-S. Hong, M. Mohseni, J. Mol. Catal. A: Chem. 242 (2005) 135–140.
[34] M.K. Seery, R. George, P. Floris, S.C. Pillai, J. Photochem. Photobiol. A: Chem. 189 (2007) 258–263.
[35] C. Sahoo, A.K. Gupta, A. Pal, Desalination 181 (2005) 91–100.
[36] H.E. Chao, Y.U. Yun, H.U. Xingfang, A. Larbot, J. Eur. Ceram. Soc. 23 (2003) 1457–1464.
[37] V. Iliev, D. Tomova, L. Bilyarska, A. Eliyas, L. Petrov, Appl. Catal. B: Environ. 63 (2006) 266–271.
[38] P. Kluson, H. Luskova, T. Cajthaml, O. Solcova, Thin Solid Films 495 (2006) 18–23.
[39] K. Koči, L. Obalová, L. Matějová, D. Plachá, Z. Lacný, J. Jirkovský, O. Šolcová, Appl. Catal. B: Environ. 89 (2009) 494–502.
[40] M.M. Ballari, R. Brandi, O. Alfano, A. Cassano, Chem. Eng. J. 136 (2008) 50–65.
[41] M.M. Ballari, R. Brandi, O. Alfano, A. Cassano, Chem. Eng. J. 136 (2008) 242–255.
[42] K. Koči, L. Obalová, D. Plachá, Z. Lacný, Coll. Czech. Chem. Commun. 73 (2008) 1192–1204.
[43] J.-M. Herrmann, J. Disdier, P. Pichat, J. Phys. Chem. 90 (1986) 6028–6034.
[44] A. Henglein, J. Phys. Chem. 83 (1979) 2209–2216.
[45] K. Shiba, H. Hinode, M. Wakihara, React. Kinet. Catal. Lett. 64 (1998) 281–288.